

Experimental Results and Mechanistic Insights on the Reactions of Indolymethyl Acetates with Soft Carbon Pronucleophiles

Antonio Arcadi, Massimiliano Aschi, Marco Chiarini, Giancarlo Fabrizi,* Andrea Fochetti, Antonella Goggiamani, Federica Iavarone, Antonia Iazzetti,* Andrea Serraiocco, and Roberta Zoppoli



Cite This: *ACS Omega* 2024, 9, 28450–28462



Read Online

ACCESS |



Metrics & More

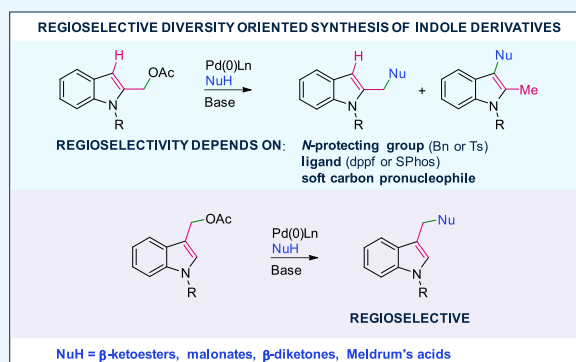


Article Recommendations



Supporting Information

ABSTRACT: The palladium-catalyzed reaction of *N*-protected 2-indolymethyl acetates with soft carbon pronucleophiles is described. Besides the formation of the expected coupling reaction at the C1' position, unprecedented attack at the C3 position of the plausible η^3 -indolyl-palladium intermediate has been observed, and the selectivity control C1'/C3 seems to depend on the nature of the protecting group and ligand. The reactivity of 3-indolymethyl acetates has also been investigated. Quantum chemical calculations support the experimental results.



INTRODUCTION

The wide spectrum of applications in medicinal chemistry, dye industry, material science, and agriculture of indoles continues to render the development of diversity-oriented synthesis of these scaffolds a very active research area.¹ In particular, the functionalization of the preformed indole ring with groups prone to undergo easy further elaboration represents a powerful tool to approach a variety of synthetic targets of great relevance in drug discovery.² Significantly, the use of indole-2-carbinols and indole-3-carbinols³ and derivatives⁴ as starting building blocks found wide applications for the preparation of chiral indole-based heterocycles.⁵ In this context, we described the functionalization of benzofurans through Tsuji–Trost-type reactions involving a palladium-catalyzed benzylic-like nucleophilic substitution exclusively at the exomethyl position (Scheme 1a).⁶ The palladium-catalyzed reaction of indolymethyl or benzofuranylmethyl acetates with boronic acids accomplished an easy approach to indole/benzofuran-containing diarylmethanes (Scheme 1b).⁷

Functionalization of the (1*H*-indol-2-yl)methyl acetates with N, O, and S soft nucleophiles and (1*H*-indol-3-yl)methyl acetates with secondary amines under metal-free conditions could also occur. Very likely, activated carbinols should be respectively precursors of transient indole methides I and II that could be trapped by different nucleophiles. ESI-MS and IR multiple-photon dissociation (IRMPD) spectroscopy analysis provided evidence about a conjugate addition of the nucleophile to 2-alkylideneindolenines I and 3-alkylideneindoleninium II (Scheme 2).⁸

Furthermore, as part of our ongoing interest in the synthesis of nitrogen-containing polycyclic scaffolds, we explored the sequential reactions of **1** with α -amino acids to afford 3-substituted 2,3-dihydropyrazino[1,2-*a*]indol-4(1*H*)-ones **2** (Scheme 3a).⁹ Analogously, the domino palladium-catalyzed reaction of indol-2-ylmethyl acetates with 1,3-dicarbonyls achieved the synthesis of 1,2-dihydro-3*H*-pyrrolo[1,2-*a*]indol-3-ones **3** (Scheme 3b).¹⁰

We envisaged that the reaction of suitable *N*-substituted-(1*H*-indolyl)methyl acetates **4** and **8** with carbon soft pronucleophiles can achieve the diversity-oriented synthesis of the corresponding indole derivatives (Scheme 4).

Although it is well-known that these types of substrates could generate the η^3 -indolyl-palladium intermediate or alkylideneindolenines, to the best of our knowledge the functionalization with β -ketoesters, 1,3-dicarbonyl compounds, malonates, and Meldrum's acids has not been examined in detail.¹¹

We supposed that computational studies could have accomplished insights into the different reaction pathways, helping to address the product selectivity control and highlighting the key role of the palladium catalysis for the reaction outcome.

Herein we report the results of our investigation.

Received: March 12, 2024

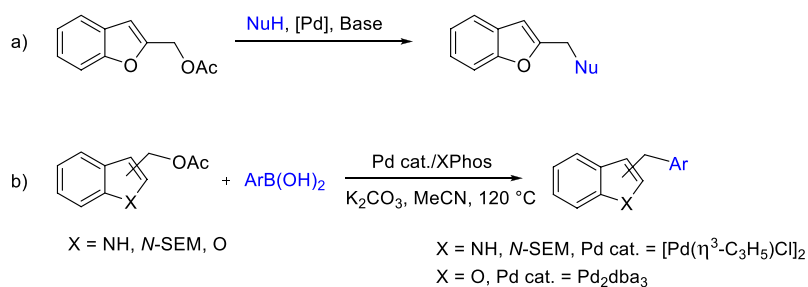
Revised: April 15, 2024

Accepted: April 19, 2024

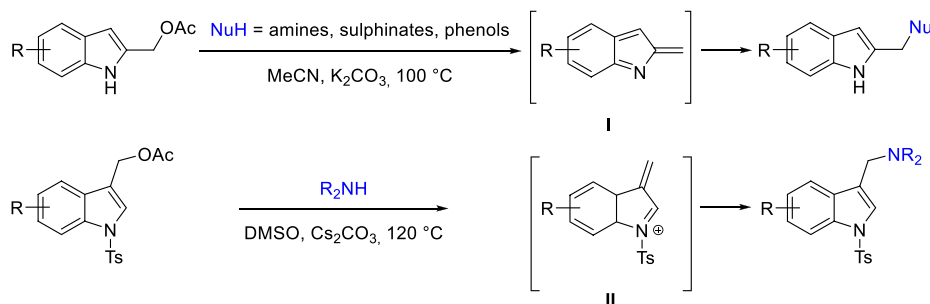
Published: June 17, 2024



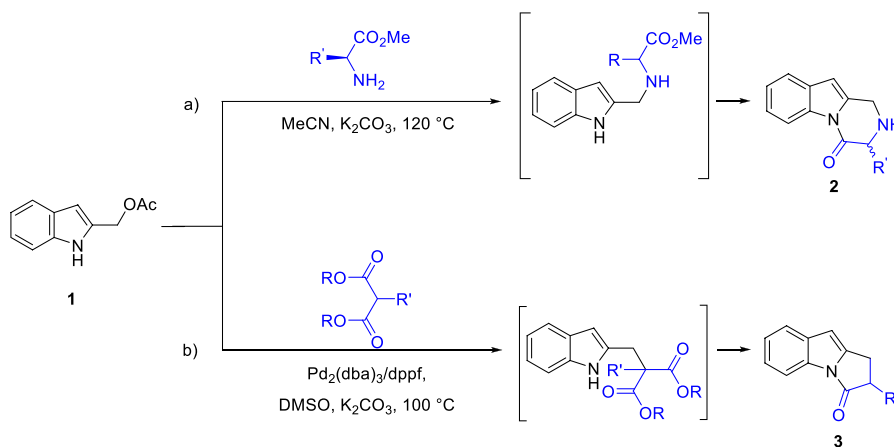
Scheme 1. (a) Benzofuran Functionalization through Palladium-Catalyzed Tsuji–Trost-Type Reactions; (B) Palladium-Catalyzed Reaction of Indolylmethyl or Benzofuranymethyl Acetates with Boronic Acids



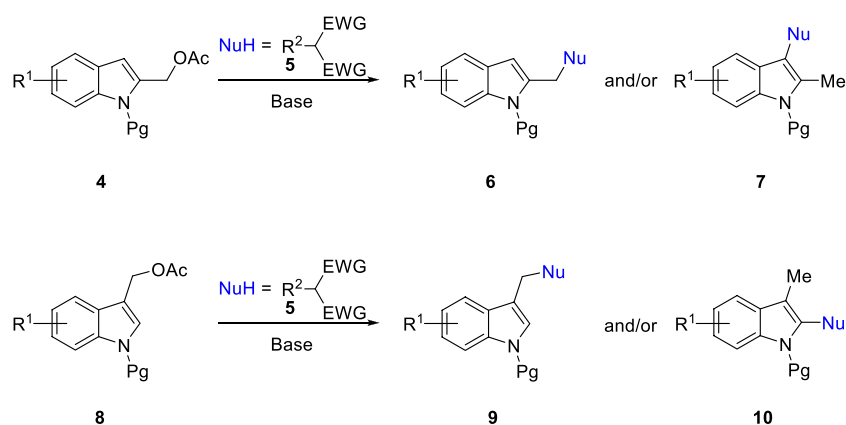
Scheme 2. Conjugate Addition-Type Reactions of Nucleophiles to the in Situ Generated Alkylideneindolenines I and Alkylideneindolinium Ions II



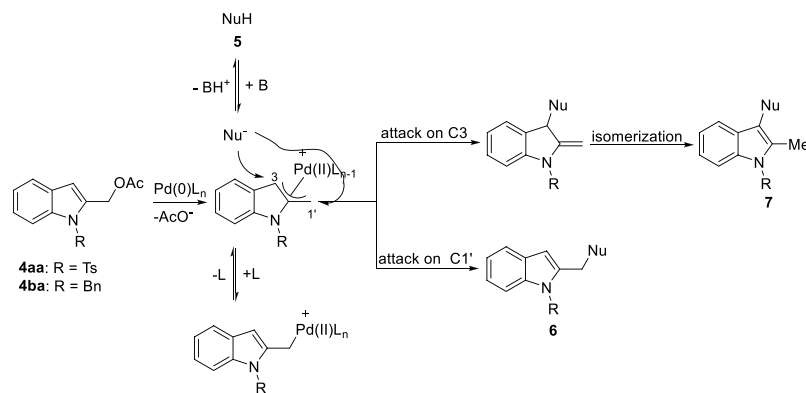
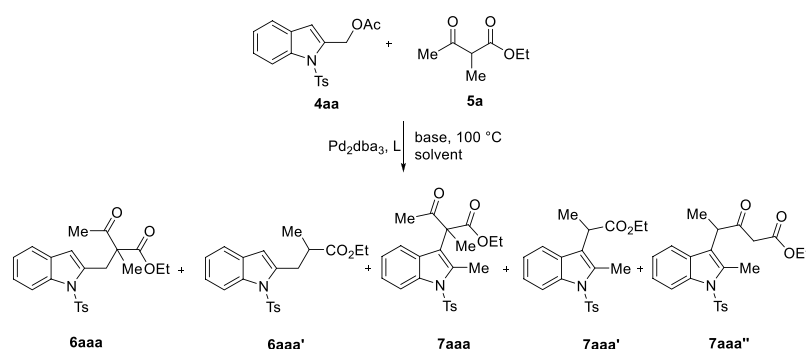
Scheme 3. Base-Promoted (a) and Palladium-Catalyzed (b) Domino Reactions of 2-Indolylmethyl Acetates 1 with α -Amino Acids and 1,3-Dicarbonyls, Respectively



Scheme 4. Present Work

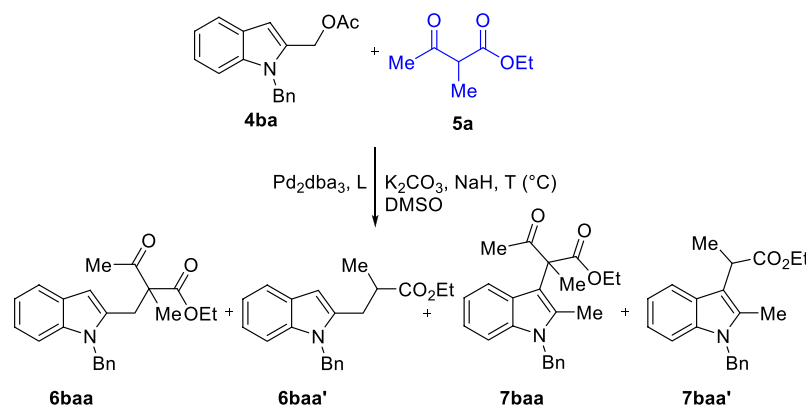


Scheme 5. C1' vs C3 Nucleophilic Attack

Table 1. Optimization Studies for the Reaction of 4aa with Ethyl 2-Methyl-3-oxobutanoate 5a^a

Entry ^b	Ligand	Solvent	Base	<i>t</i> (h)	6aaa (%)	6aaa' (%)	7aaa (%)	7aaa' (%)	7aaa'' (%)	Overall yield (%)	C1'/C3
1	dppf	DMSO	Li ₂ CO ₃	24	0	5	0	1		6	83/17
2	dppf	DMSO	Cs ₂ CO ₃	5	27	19	21	8		75	60/40
3	dppf	DMSO	K ₂ CO ₃	24	19	21	19	8		67	60/40
4	dppf	THF	NaH	5.5	13	2	3	1		19	74/26
5	dppf	THF	K ₂ CO ₃ /NaH	24	0	37	0	12		49	75/25
6	dppf	DMF	NaH	24	29	3	33	1	traces	66	49/51
7	dppf	DMF	K ₂ CO ₃ /NaH	24	32	8	36	5	traces	81	49/51
8	dppf	DMSO	K ₂ CO ₃ /NaH	24	31	14	34	6	13	98	46/54
9	dppm	DMSO	K ₂ CO ₃ /NaH	24							
10	dppe	DMSO	K ₂ CO ₃ /NaH	24	34	6	16	3	6	65	67/33
11	dppp	DMSO	K ₂ CO ₃ /NaH	4	54	6	30		10	100	60/40
12	XantPhos	DMSO	K ₂ CO ₃ /NaH	3.5	16	5	56	7	16	100	21/79
13	DavePhos	DMSO	K ₂ CO ₃ /NaH	3	16	8	53	5	17	99	24/76
14	XPhos	DMSO	K ₂ CO ₃ /NaH	64	6		28		8	42	14/86
15 ^c	DavePhos	DMSO	K ₂ CO ₃ /NaH	2	10	1	41	6	6	67	30/70
16 ^{c,d}	DavePhos	DMSO	K ₂ CO ₃ /NaH	26	5	6	15	7		33	33/67
17	RuPhos	DMSO	K ₂ CO ₃ /NaH	3	12	5	43	9	12	81	27/73
18	SPhos	DMSO	K ₂ CO ₃ /NaH	3	11		55	8	17	92	12/88
19	MePhos	DMSO	K ₂ CO ₃ /NaH	24		12		8		20	74/26
20	JohnPhos	DMSO	K ₂ CO ₃ /NaH	24	2	9	8	7		26	59/41
21	(<i>o</i> -furyl) ₃ P	DMSO	K ₂ CO ₃ /NaH	24							
22	TTTP	DMSO	K ₂ CO ₃ /NaH	3.5	31	3	39	3	24	100	34/66
23	(<i>t</i> -Bu) ₃ PHBF ₄	DMSO	K ₂ CO ₃ /NaH	24	4	11				15	100/0
24	<i>t</i> -BuXPhos	DMSO	K ₂ CO ₃ /NaH	24		3		3		6	87/13
25	<i>t</i> -BuXantPhos	DMSO	K ₂ CO ₃ /NaH	24		8		2		10	93/7

^aUnless otherwise stated, reactions were carried out on a 0.30 mmol scale under an argon atmosphere using 0.02 equiv of Pd₂dba₃, 0.08 equiv of monodentate ligand or 0.04 of bidentate ligand, 1.5 equiv of 5a, 1.5 equiv of M₂CO₃ and 1.7 equiv of NaH when present in 2.5 mL of anhydrous solvent at 100 °C. ^bYields are given for isolated products. ^cReaction was carried out with [Pd(C₃H₅)Cl]₂. ^dReaction was carried out with preformed sodium salt of 5a.

Table 2. Reaction of 4ba with Ethyl 2-Methyl-3-oxobutanoate 5a^a

Entry ^b	Ligand	T (°C)	t (h)	6baa (%)	6baa' (%)	7baa (%)	7baa' (%)	Overall yield (%)	C1'/C3
1	dppp	120	24	31	51	2		84	97/3
2	dppp	100	24	44	49	3		96	97/3
3	dppf	100	2	53	42	3		98	97/3
4	DavePhos	120	24	2	53	3		57	96/4
5 ^c	SPhos	100	3	47	36	5		88	96/4

^aUnless otherwise stated, reactions were carried out on a 0.30 mmol scale under an argon atmosphere using 0.02 equiv of Pd₂dba₃, 0.08 equiv of monodentate ligand or 0.04 of bidentate ligand, 1.5 equiv of 5a, 1.5 equiv of K₂CO₃, and 1.7 equiv of NaH in 2.5 mL of anhydrous DMSO. ^bYields are given for isolated products. ^c4ba was recovered in 12% yield.

RESULTS AND DISCUSSION

To prevent the formation of 1,2-dihydro-3H-pyrrolo[1,2-a]indol-3-ones **3** previously reported by us (Scheme 3b),¹⁰ we started our investigation by exploring the palladium-catalyzed reaction of *N*-protected (1*H*-indol-2-yl)methyl acetate **4** with ethyl 2-methyl-3-oxobutanoate **5a**. Surprisingly, with (1-tosyl-1*H*-indol-2-yl)methyl acetate **4aa** we observed that, besides the formation of the expected coupling reaction at the C1' position, an unprecedented attack at the C3 position of the plausible η³-indolyl-palladium intermediate can occur (Scheme 5).

With the aim to achieve product selectivity control, we tested the reaction using a variety of ligands, bases, and solvents (Table 1). Ligands showed significant influence on the reactivity and selectivity. The bidentate bisphosphine ligand dppf was effective in allowing the conversion of the starting **4aa** up to 98% with the formation of the substitution products in C1'/C3 ratio 46/54 when the reaction was carried out in DMSO at 100 °C in the presence of a mixture of K₂CO₃/NaH (Table 1, entry 8). Poorer conversion was observed when Cs₂CO₃ or K₂CO₃ was used as a base under the same reaction conditions (Table 1, entries 2 and 3) while Li₂CO₃ was found to be ineffective (Table 1, entry 1). Comparable results were observed when DMF was used instead of DMSO (Table 1, entries 6 and 7), but THF was unsuitable, although it achieved a better C1' selectivity (Table 1, entries 4 and 5). The use also of only NaH in DMF gave poorer conversion compared to the use of the mixture of K₂CO₃/NaH under the same conditions (Table 1, entry 6 vs entry 7). Up to quantitative conversion of the starting **4aa** was observed when the reaction with ethyl 2-methyl-3-oxobutanoate **5a** (1.5 equiv) was carried out in DMSO at 100 °C in the presence of K₂CO₃ (1.5 equiv), NaH (1.7 equiv), Pd₂(dba)₃ (0.08 equiv), and the bidentate ligand dppp (0.04 equiv) (Table 1, entry 11). While dpmm was ineffective (Table 1, entry 9), the comparison with the results observed with the use of dppe instead of dppp (Table 1, entries 10 and 11) highlighted the importance of a wide bite angle of the ligand on the reactivity and regioselectivity. Indeed,

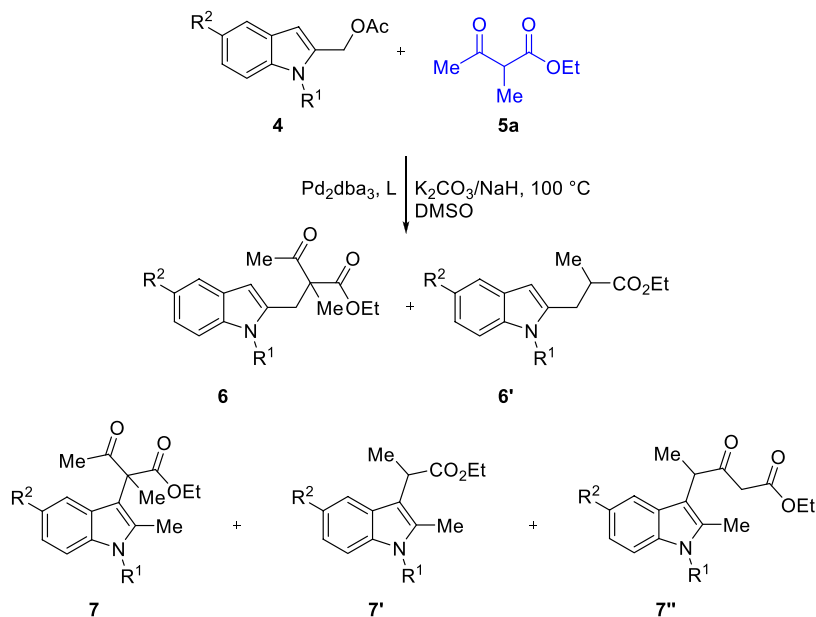
the use of bulkier Xantphos achieved, besides the quantitative conversion of **4aa**, the reversion of the regioselectivity toward the prevalent formation of the C3-substituted products (Table 1, entry 12). Similar switching of the regioselectivity toward the C3-substituted products resulted when the reaction occurred in the presence of monophosphine ligands bearing a dialkyl biaryl framework (Table 1, entries 13–18) in contrast with those obtained in the presence of MePhos and JohnPhos (Table 1, entries 19 and 20). The employment of [Pd(η³-C₃H₃)Cl]₂ with DavePhos instead of Pd₂dba₃ was also attempted (Table 1, entries 15 and 16). However, both steric and electronic properties of the ligands determined the reactivity and the regioselective outcome (Table 1, entries 21–25).¹² The formation of the products **6aaa'** and **7aaa'** should derive from a retro Claisen reaction under the reaction conditions.¹³

Subsequently, we used *N*-benzyl derivative **4ba** to explore the effect of a different *N*-protective group on the control of the regioselective outcome. In all cases examined, we observed high regioselective formation of products functionalized at the C1' position in high overall yield (Table 2).

When the optimized reaction conditions [Pd₂dba₃, SPhos or dppf, K₂CO₃, and NaH in anhydrous DMSO] were extended to a variety of functionalized (*N*-substituted-1*H*-indol-2-yl)methyl acetate **4**, comparative experiments demonstrated the influence of the *N*-benzyl group on directing the regioselective outcome regardless of the feature of the substituent on the aryl ring of the starting acetate (Table 3).

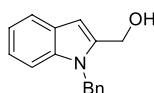
The study of the influence of the feature of the carbon soft pronucleophile on the reaction outcome showed that the reaction of the *N*-benzyl derivative **4ba** with the 2-methylethylmalonate **5b** afforded only the C1'-substituted products in moderate yield under the standardized reaction conditions [Pd₂dba₃, SPhos or dppf, K₂CO₃, and NaH in anhydrous DMSO] while the regioselectivity control failed to occur with the more reactive *N*-tosyl derivative **4aa** (Table 4).

By contrast, both compounds **6bac** (Table 5, entry 2) and **6aac** (Table 5, entry 6) were isolated in satisfactory yield

Table 3. Reaction of Functionalized Derivatives 4 with Ethyl 2-Methyl-3-oxobutanoate 5a^a

Entry ^b	R ¹	R ²	4	Ligand	t (h)	6 (%)	6' (%)	7 (%)	7' (%)	7'' (%)	Overall yield (%)	C1'/C3
1	Bn	Cl	4bb	dppf	1	6bba (79)	6bba' (9)	7bba (/)	7bba' (/)	7bba'' (/)	88	100/0
2	Ts	OMe	4ab	dppf	2	6aba (44)	6aba' (4)	7aba (26)	7aba' (3)	7aba'' (8)	85	57/43
3 ^c	Ts	OMe	4ab	SPhos	24	6aba (10)	6aba' (9)	7aba (18)	7aba' (13)	7aba'' (3)	53	38/62
4	Bn	OMe	4bc	dppf	2	6bca (46)	6bca' (15)	7bca (/)	7bca' (/)	7bca'' (/)	71	100/0
5	Ts	Me	4ac	dppf	20	6aca (36)	6aca' (17)	7aca (36)	7aca' (4)	7aca'' (8)	100	53/47
6	Ts	Me	4ac	Sphos	20	6aca (14)	6aca' (10)	7aca (46)	7aca' (20)	7aca'' (7)	98	25/75
7 ^d	Bn	Me	4bd	dppf	1	6bda (40)	6bda' (21)	7bda (/)	7bda' (/)	7bda'' (/)	61	100/0
8	Ts	Ph	4ad	dppf	6	6ada (24)	6ada' (3)	7ada (38)	7ada' (4)	7ada'' (7)	76	35/65
9	Bn	Ph	4be	dppf	3	6bea (86)	6bea' (13)	7bea (/)	7bea' (/)	7bea'' (/)	99	100/0

^aUnless otherwise stated, reactions were carried out on a 0.30 mmol scale under an argon atmosphere using 0.02 equiv of Pd₂dba₃, 0.08 equiv of SPhos or 0.04 of dppf, 1.5 equiv of 5a, 1.5 equiv of K₂CO₃, and 1.7 equiv of NaH in 2.5 mL of anhydrous DMSO. ^bYields are given for isolated products. ^c4ab was recovered in 5% yield. ^d(1-Benzyl-1H-indol-2-yl)methanol 11ba was isolated in 5% yield.



11ba

through the palladium-catalyzed reaction of the indolylmethyl acetates 4aa–4ba with the methyl Meldrum's acid 5c via sequential attack of the corresponding enolate at the C1' position/elimination of acetone and CO₂ (Table 5).¹⁴

Interestingly, the heptanoic acid derivatives 13a,b were effectively obtained under optimized reaction conditions (Table 6, entries 2 and 4) through the sequential C1' regioselective substitution/retro-Dieckmann reactions of acetates 4 with 2-methylcyclohexane-1,3-dione 5d.¹⁵ Only traces of 2-methyl-2-((1-tosyl-1H-indol-2-yl)methyl)cyclohexane-1,3-dione 6aad were detected (Table 6, entry 5).

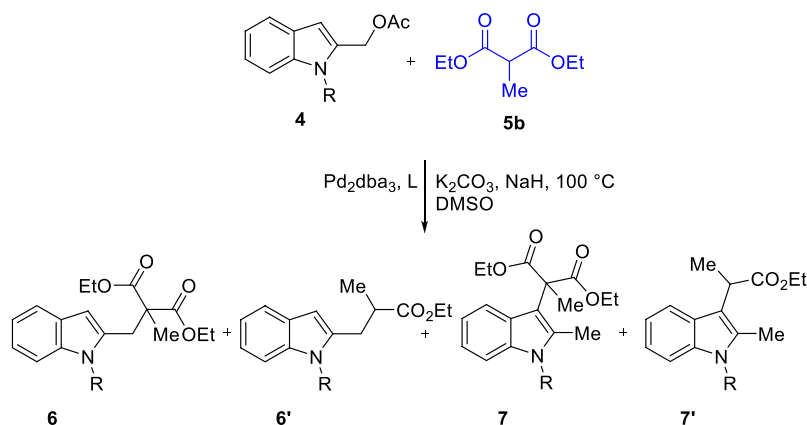
The potential of the strategy aimed at the diversity-oriented synthesis of indole derivatives is further highlighted by the investigation of the palladium-catalyzed regioselective functionalization of (1-substituted-1H-indol-3-yl)methyl acetates 8a with a variety of carbon pronucleophiles. Indeed, ethyl 2-methyl-3-oxo-2-((1-tosyl-1H-indol-3-yl)methyl)butanoate 9aa was isolated in 98% yield by reacting acetate 8a in MeCN in the presence of Pd₂dba₃/dppf as the catalytic system (Table 7, entry 5) or by carrying out the reaction using [Pd(η³-C₃H₅)Cl]/XPhos and 3 equiv of 5a at 120 °C in a mixture 4:1 of MeCN/

THF solvents (Table 7, entry 4). The formation of the product by a base-promoted reaction can be ruled out by recovering the starting acetate under metal-free conditions (Table 7, entry 1). The choice of the suitable reaction medium also achieved the suppression of the retro Claisen reaction, leading to the conversion of 9aa to ethyl 2-methyl-3-(1-tosyl-1H-indol-3-yl)propanoate 9aa' which prevailed as the main product in a 4:1 DMSO/THF mixture of solvent (Table 7, entry 3).

Furthermore, after a brief screening with 8a and ethyl 2-methylmalonate 5b, we found that the best conditions were the same as used with 5a [Pd₂dba₃, XPhos, and K₂CO₃ in MeCN/THF] (Table 8, entry 6). After prolonged reaction times, the hydrolysis of the tosyl group can also be observed to some extent (Table 8, entries 3–5).

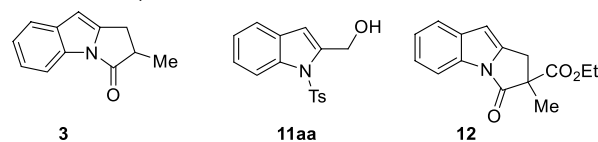
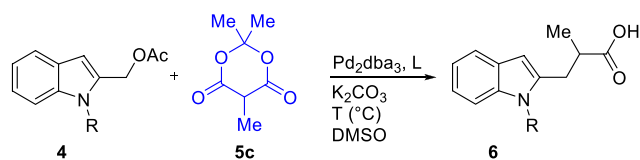
Then, the substituted *N*-Ts-indol-3-ylmethyl acetates 8 reacted under the standardized reaction conditions with the β-ketoesters and malonates 5a–g to afford the corresponding products 9 in moderate to high yield (Table 9).

A brief exploration of the palladium-catalyzed reaction of *N*-Ts-indol-3-ylmethyl acetates showed that the reaction of 8 with diketones 5d and 5h gave the corresponding 2-methyl-2-(1-

Table 4. Reaction of Functionalized Derivatives 4 with 2-Methylethyl Malonate 5b^a

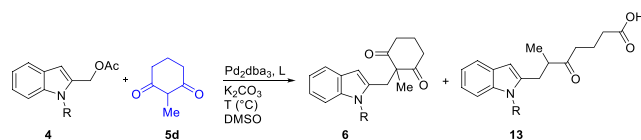
Entry ^b	R	4	Ligand	t (h)	6 (%)	6' (%)	7 (%)	7' (%)	Overall yield (%)	C1'/C3
1 ^{c,d}	Bn	4ba	dppf	24	6bab (39)	6baa' (7)	7bab (/)	7baa' (/)	46	100/0
2 ^e	Bn	4ba	SPhos	24	6bab (27)	6baa' (26)	7bab (/)	7baa' (/)	53	100/0
3 ^{f,g,h}	Ts	4aa	dppf	24	6aab (29)	6aaa' (3)	7aab (35)	7aaa' (/)	84	58/42
4 ^{h,i,j}	Ts	4ba	SPhos	5	6aab (18)	6aaa' (/)	7aab (43)	7aaa' (/)	88	51/49

^aUnless otherwise stated, reactions were carried out on a 0.30 mmol scale under an argon atmosphere using 0.02 equiv of Pd₂dba₃, 0.08 equiv of ligand, 1.5 equiv of 5b, 1.5 equiv of K₂CO₃, and 1.7 equiv of NaH in 2.5 mL of anhydrous DMSO. ^bYields are given for isolated products. ^c(1-Benzyl-1*H*-indol-2-yl)methanol 11ba was isolated in 17% yield. ^d4ba was recovered in 12% yield. ^e(1-benzyl-1*H*-indol-2-yl)methanol 11ba was isolated in 11% yield. ^f3 was isolated in 12% yield. ^g12 was isolated in 5% yield. ^hOverall yield and C1'/C3 ratio were calculated including 3 and 12. ⁱ3 was isolated in 16% yield. ^j12 was isolated in 11% yield.

Table 5. Reaction of Functionalized Derivatives 4 with Methyl Meldrum's Acid 5c^a

Entry ^b	R	4	Ligand	T (°C)	t (h)	6 (%)
1 ^c	Bn	4ba	dppf	100	24	6bac (/)
2 ^d	Bn	4ba	dppf	120	9	6bac (60)
3 ^{e,f}	Ts	4aa		100	24	6aac (/)
4 ^{e,g,h}	Ts	4aa		120	24	6aac (/)
5 ^{i,j}	Ts	4aa	dppf	100	72	6aac (/)
6	Ts	4aa	dppf	120	2	6aac (62)
7 ^k	Ts	4aa	dppf	120	24	6aac (20)
8	Ts	4aa	XantPhos	120	24	6aac (31)
9 ^{l,m}	Ts	4aa	SPhos	120	42	6aac (18)

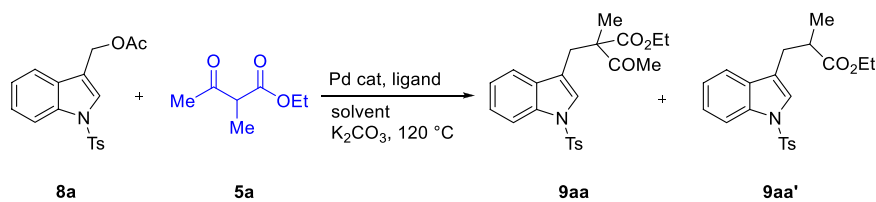
^aUnless otherwise stated, reactions were carried out on a 0.30 mmol scale under an argon atmosphere using 0.02 equiv of Pd₂dba₃, 0.08 equiv of ligand, 1.5 equiv of 5c, and 1.5 equiv of K₂CO₃ in 2.5 mL of anhydrous DMSO. ^bYields are given for isolated products. ^c4ba was recovered in 77% yield. ^d4ba was recovered in 5% yield. ^eThe reaction was carried out without Pd₂dba₃. ^f4aa was recovered in 80% yield. ^g4aa was recovered in 37% yield. ^h1-Tosyl-1*H*-indol-2-yl)methanol 11aa was isolated in 6% yield. ⁱ4aa was recovered in 77% yield. ^j3 was isolated in 8% yield. ^kReaction was carried out in the presence of Cs₂CO₃. ^l4aa was recovered in 16% yield. ^m3 was isolated in 18% yield.

Table 6. Reaction of Functionalized Derivatives 4 with 2-Methylcyclohexane-1,3-dione 5d^a

Entry ^b	R	4	Ligand	T (°C)	t (h)	13 (%)
1 ^c	Bn	4ba	dppf	120	3	13b (68)
2 ^d	Ts	4aa	dppf	120	72	13a (27)
3 ^e	Ts	4aa	dppf	100	72	13a (20)
4 ^c	Ts	4aa	dppf	100	24	13a (64)
5 ^{c,f}	Ts	4aa	dppf	120	2	13a (19)
6 ^{c,g}	Ts	4aa	SPhos	100	18	13a (/)

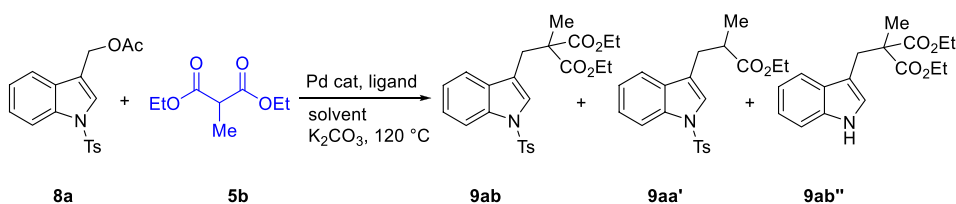
^aUnless otherwise stated, reactions were carried out on a 0.30 mmol scale under an argon atmosphere using 0.02 equiv of Pd₂dba₃, 0.08 equiv of SPhos or 0.04 equiv of dppf, 1.5 equiv of 5d, and 1.5 equiv of K₂CO₃ in 2.5 mL of anhydrous DMSO. ^bYields are given for isolated products. ^cThe reaction was carried out with potassium salt of 5d. ^d4aa was recovered in 40% yield. ^e4aa was recovered in 40% yield. ^f6aad was detected in traces. ^g4aa was recovered in 54% yield.

tosyl-1*H*-indol-3-yl)methyl)cyclohexane-1,3-dione 9ad and 3-methyl-3-(1-tosyl-1*H*-indol-3-yl)methyl)pentane-2,4-dione 9ah in 91% and 80% yields, respectively (Table 10, entries 1 and 2). The presence of chlorine on the benzene ring as substituent is well tolerated, while the methoxy group determined an increase in the amount of the retro Claisen derivative 9' (Table 10, entries 3 and 4).

Table 7. Optimization Studies for the Reaction of 11a with Ethyl 2-Methylacetoacetate 5a^a

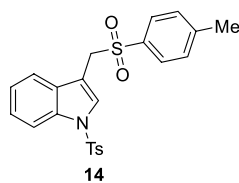
Entry ^b	Pd cat.	Ligand	Solvent	t (h)	9aa (%)	9aa' (%)
1 ^c			DMSO	5	9	
2	Pd ₂ (dba) ₃	dppf	DMSO	2	75	9
3	Pd ₂ (dba) ₃	SPhos	DMSO/THF 4:1	24	20	49
4	[Pd(C ₃ H ₅)Cl] ₂	XPhos	MeCN/THF 4:1	24	98	
5	Pd ₂ (dba) ₃	dppf	MeCN	8	98	

^aUnless otherwise stated, reactions were carried out on a 0.29 mmol scale under an argon atmosphere using 0.04 equiv of Pd, 0.04 equiv of ligand, 3 equiv of 5a, and 2 equiv of K₂CO₃ in 2.5 mL of anhydrous solvent at 120 °C. ^bYields are given for isolated products. ^c8a was recovered in 53%

Table 8. Optimization Studies for the Reaction of 8a with Ethyl 2-Methylmalonate 5b^a

Entry ^b	Pd cat.	Ligand	Solvent	t (h)	9ab (%)	9aa' (%)	9ab'' (%)
1	Pd ₂ (dba) ₃	dppf	DMSO	4	55	6	
2 ^c	Pd ₂ (dba) ₃	dppf	MeCN	2	84	9	
3 ^d	Pd ₂ (dba) ₃	dppf	1,4-dioxane	29	41	49	4
4	[Pd(C ₃ H ₅)Cl] ₂	SPhos	DMSO/THF 4:1	29	45	14	11
5 ^e	[Pd(C ₃ H ₅)Cl] ₂	SPhos	MeCN/THF 4:1	8	69		11
6	[Pd(C ₃ H ₅)Cl] ₂	XPhos	MeCN/THF 4:1	2.5	81		

^aUnless otherwise stated, reactions were carried out on a 0.29 mmol scale under an argon atmosphere using 0.04 equiv of Pd, 0.04 equiv of ligand, 2 equiv of 5b, and 2 equiv of K₂CO₃ in 2.5 mL of anhydrous solvent. ^bYields are given for isolated products. ^c14 was isolated in 7%. ^d14 was isolated in 15% yield. ^e14 was isolated in 8% yield.



Finally, the study of the palladium-catalyzed reaction of *N*-Ts-indol-3-ylmethyl acetates with Meldrum's acid derivatives 5c demonstrated the general effectiveness of the regioselective diversity orientated synthesis of indoles of the procedure (Table 11).

Intrigued by the experimental results of the *N*-free and *N*-protected indolylmethyl acetates with soft carbon pronucleophiles, we performed quantum-chemical calculations as reported in the Computational Details, aimed to provide insight into the reaction pathways enabling us to achieve the product selectivity control and to clarify the differences between the palladium-catalyzed vs the metal-free processes previously reported by us (Schemes 2 and 3).^{6–10}

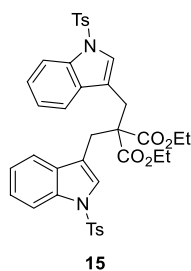
All the calculations were performed in the framework of the Density Functional Theory using the wB97XD functional, corresponding to a range-separated version of Becke's 97 functional with additional dispersion correction,¹⁶ with different basis sets: geometry optimizations were carried out with the 6-

31G* for the atoms of the first, second, and third row elements, the Los Alamos Effective Core Potential with a double- ζ basis set (LANL2DZ) was used for palladium.¹⁷ Energies were then refined through single point calculations, adding a diffusion function (6-31+G*) to the second and third row elements. All the structures were optimized in the gas phase and characterized, through the calculation of the mass-weighted Hessian matrix, as minima (all positive eigenvalues of the Hessian matrix) or transition structures (1 negative eigenvalue of the Hessian matrix). The Gibbs molar free energy ($G_{X,\text{gas}}$) was then calculated, using the previous geometries and harmonic frequencies, for each species in the gas phase at 100 °C and at the concentration of 1.0 mol/L (standard state) using the standard statistical-mechanical relations. Finally the solvation in DMSO, i.e., excess molar free energy ($G_{X,\text{solv}}$), was calculated within the mean-field approximation in DCE using the Polarizable Continuum Model (PCM).¹⁸ Within this approximation, the molar free energy (G_X) for the generic X species in

Table 9. Reaction of *N*-Ts-indol-3-ylmethyl Acetates **8** with β -Ketoester and Malonates **5**^a

Entry ^b	Catalytic system	R ¹	8	5	t (h)	9 (%)
					5.5	9be (80)
1	A	5-NO ₂	8b		5e	
2 ^c	A	5-NO ₂	8b		5f	9bf (87)
3	A	5-OMe	8c		5e	9ce (82)
	B				32	9ce (89)
4	A	5-OMe	8c		5f	9cf (93)
5	A	5-OMe	8c		5a	9ca (99)
6 ^d	A	6-Cl	8d		5e	9de (27)
	B				25	9de (77)
7 ^e	A	6-Cl	8d		5f	9df (30)
	B				6	9df (80)
8	B	6-Cl	8d		5a	9da (90)
9	A	5-NO ₂	8b		5b	9bb (79)
10	A	5-OMe	8c		5b	9cb (78)
11 ^f	A	6-Cl	8d		5b	9db (55)
12	B				24	9db (77)
13 ^g	A	H	8a		5g	9ag (59)
14	A	H	8a		5e	9ae (87)
15	A	H	8a		5f	9af (91)

^aUnless otherwise stated, reactions were carried out on a 0.29 mmol scale under an argon atmosphere at 100 °C using 2.0 equiv of **5**, 0.025 equiv of [Pd(C₃H₅Cl)₂], 0.05 equiv of XPhos, and 2 equiv of K₂CO₃ in 2.5 mL of MeCN/THF mixture (4:1) [Condition A] or 0.025 equiv of [Pd(C₃H₅Cl)₂] and 0.025 equiv of dppf in MeCN [Condition B]. ^bYields are given for isolated products. ^c**8c** was recovered in 10% yield. ^d**8c** was recovered in 56% yield. ^e**8d** was recovered in 24% yield. ^f**8d** was recovered in 9% yield. ^g**15** was isolated in 12% yield.



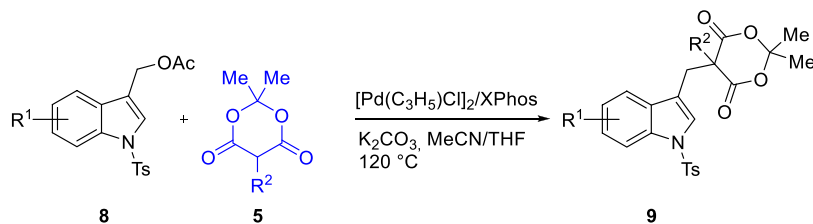
solution was simply evaluated through the usual equation $G_X = G_{X,\text{gas}} + G_{X,\text{solv}} + RT \ln [X]$. Of course, in the standard state reported in all the figures, $[X] = 1.0$ M for all the species in solution. All the quantum-chemical calculations were carried out with the Gaussian09 package.¹⁹ All the Cartesian coordinates of the optimized geometries are collected in the [Supporting Information](#).¹⁹ First of all we have modeled the initial stage of

the C1' vs C3 nucleophilic attack on the indolyl-palladium intermediate (see [Scheme 5](#)). For this purpose, we have utilized 2-methylmalonaldehyde **5l** as nucleophile, two PH₃ groups as simplified palladium ligands, and three different *N*-substituents (R = H, Ts, and Bn). The results are reported in [Figures 1](#) (R = H), [2](#) and [3](#) (R = Ts), and [4](#) (R = Bn). In all the cases, we have observed that the channel leading to the C1'-substituted

Table 10. Reaction of *N*-Ts-indol-3-ylmethyl Acetates **8** with 1,3-Diketones **5d,h**^a

Entry ^b	R ¹	8	5	t (h)	9 (%)	9' (%)
1	H	8a		1.5	9ad (91)	/
2	H	8a		1	9ah (80)	3
3	5-OMe	8c		2.5	9ch (43)	37
4	6-Cl	8d		24	9dh (71)	18

^aUnless otherwise stated, reactions were carried out on a 0.29 mmol scale under an argon atmosphere using 0.04 equiv of Pd, 0.04 equiv of ligand, 3 equiv of **5**, and 2 equiv of K₂CO₃ in 2.5 mL of anhydrous solvent. ^bYields are given for isolated products.

Table 11. Reaction of *N*-Ts-indol-3-ylmethyl Acetates **8** with Meldrum's Acid Derivatives **5**^a

Entry ^b	R ¹	8	R ²	t (h)	9 (%)
1	H	8a	Me	8	9ac (98)
2	H	8a	CH ₂ (4-OMeC ₆ H ₄)	0.5	9ai (98)
3	H	8a	CH ₂ (4-SMeC ₆ H ₄)	7	9aj (80)
4	H	8a	CH ₂ (2-furyl)	1	9ak (99)
5	5-NO ₂	8b	Me	1.5	9bc (88)
6	5-OMe	8c	Me	0.5	9cc (95)
7	5-OMe	8c	CH ₂ (4-OMeC ₆ H ₄)	0.5	9ci (95)
8	5-OMe	8c	CH ₂ (4-SMeC ₆ H ₄)	6	9cj (83)
9	5-OMe	8c	CH ₂ (2-furyl)	1.5	9ck (91)
10	6-Cl	8d	CH ₂ (4-OMeC ₆ H ₄)	25	9di (70)
11	6-Cl	8d	CH ₂ (4-SMeC ₆ H ₄)	6.5	9dj (75)
12	6-Cl	8d	CH ₂ (2-furyl)	24	9dk (89)

^aUnless otherwise stated, reactions were carried out on a 0.29 mmol scale under an argon atmosphere at 120 °C using 1.5 equiv of **5**, 0.025 equiv of [Pd(C₃H₅Cl)₂] and 0.05 equiv of XPhos, and 2 equiv of K₂CO₃ in 2.5 mL of MeCN/THF mixture (4:1). ^bYields are given for isolated products.

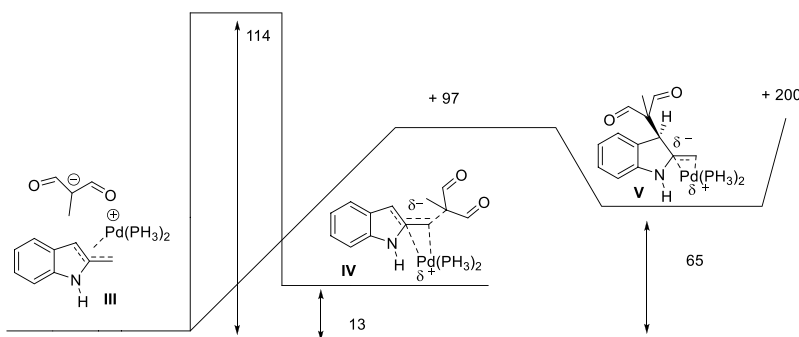


Figure 1. Standard free energy diagram (at 100 °C in DMSO) in kJ/mol.

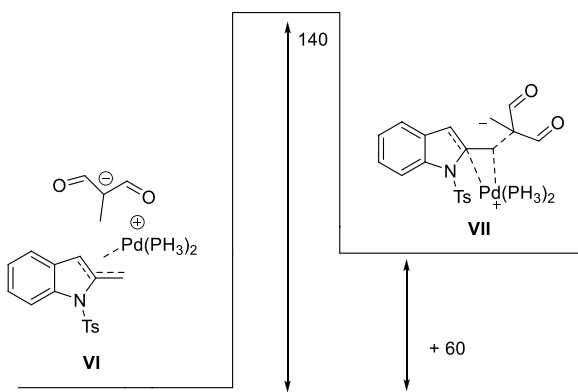


Figure 2. Standard free energy diagram (at 100 °C in DMSO) in kJ/mol.

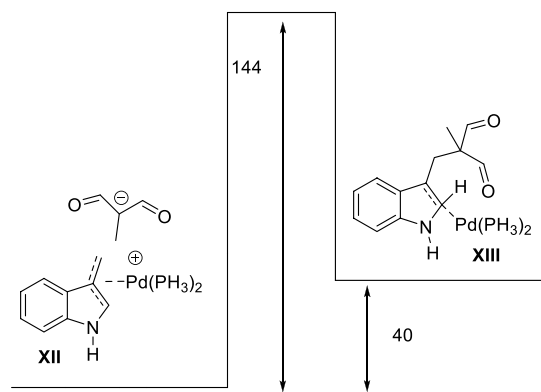


Figure 5. Standard free energy diagram (at 100 °C in DMSO) in kJ/mol.

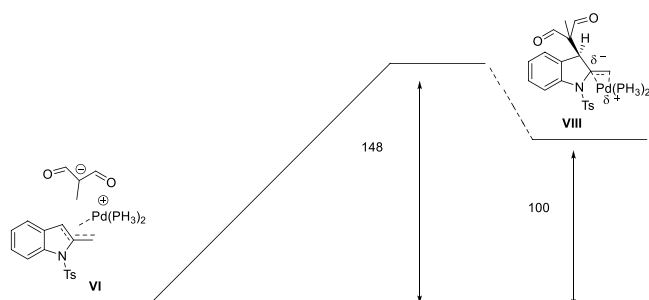


Figure 3. Standard free energy diagram (at 100 °C in DMSO) in kJ/mol.

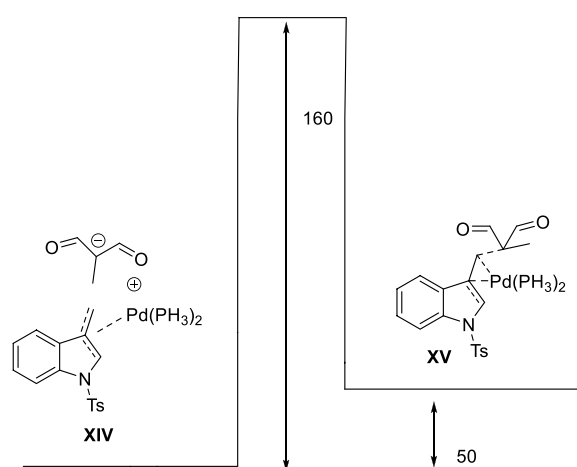


Figure 6. Standard free energy diagram (at 100 °C in DMSO) in kJ/mol.

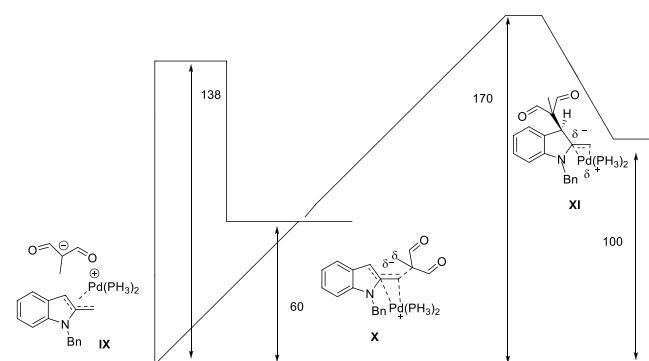


Figure 4. Standard free energy diagram (at 100 °C in DMSO) in kJ/mol.

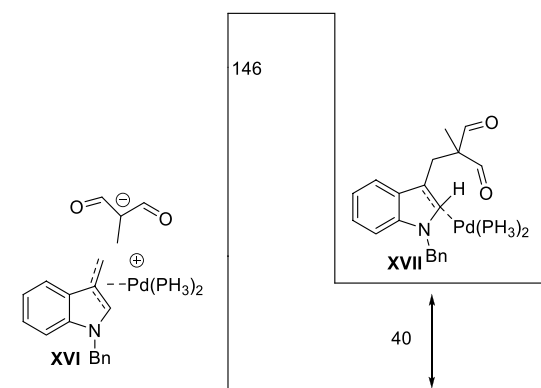


Figure 7. Standard free energy diagram (at 100 °C in DMSO) in kJ/mol.

product is the dominant one. As a matter of fact, irrespective of the height of the initial free energy barrier, the C1' attack always leads to an intermediate more stable than the intermediate expected upon C3 attack and the barrier for the 1–3 H-shift is always found to be particularly high. In particular, when R = H the formation of the thermodynamically unstable intermediate V is a reversible process, which might explain the absence of product substituted at the C3 position. When R = Ts (Figures 2 and 3) we observe that the two intermediates VII and VIII show rather similar barrier heights; on the other hand, when R = Bn (Figure 4) the formation of intermediate XI is characterized by a very high barrier, hence not in disagreement with the experimental data.

Subsequently, we repeated the same calculations for the 3-indolylmethyl-palladium intermediates. Also in this case from the results, depicted in Figures 5 (R = H), 6 (R = Ts), and 7 (R =

Bn), we can expect a very high regioselectivity of the nucleophilic attack. As a matter of fact, we observe that (i) a relatively low barrier is found only for the C₁' attack, (ii) the attack at the C₂ position does not show any transition structure, (iii) all the reaction intermediates show a similar thermodynamic stability, and (iv) all three reactions are characterized by rather similar barrier heights, slightly higher when R = Ts. All of the results are in agreement with the experimental observations.

We also addressed the question of what could be the actual role of the Pd. In Figure 8 we report the free energy diagram

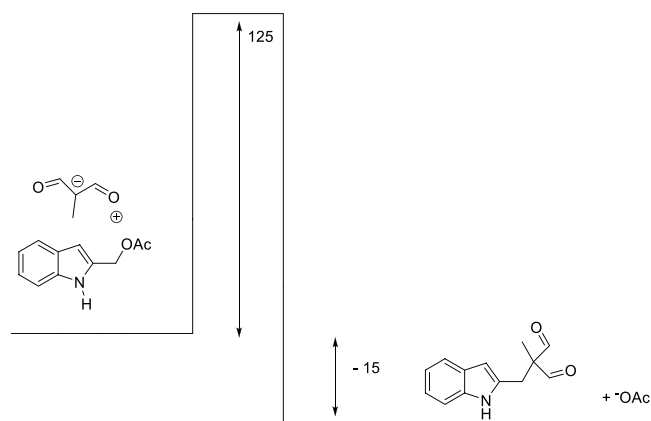


Figure 8. Standard free energy diagram (at 100 °C in DMSO) in kJ/mol.

(maintaining the same temperature and solvent conditions) for the Pd-free reaction with R = H. The result clearly indicates that, at least according to our model, the absence of Pd increases the initial free energy barrier of only 9 kJ/mol, hence suggesting the possible occurrence also of a S_N2 reaction essentially leading to the same product.

Finally, we carried out DFT calculations, in the same temperature and solvent conditions, to provide thermodynamic information concerning additional aspects that could help in rationalizing the possibility of alternative Pd-free reaction pathways involving indolymethyl cations **XVIII** and **XIX**. As reported in [Figure 9](#), the calculated relative stability, and hence the possible presence at equilibrium, of the indolymethyl cations indicate that these species under the experimental conditions modeled by our calculations show molar ratios of 4.5×10^{-5} and 3.0×10^{-3} , respectively. The same conclusions could

be reached for the possible formation of intermediate **I** by deprotonation with a Bronsted base.

CONCLUSIONS

The palladium-catalyzed reaction of *N*-protected indolymethyl acetates with different classes of soft carbon pronucleophiles has been investigated. The role of protecting groups, nucleophiles, and ligands in the selective attack on the plausible η^3 -indolyl-palladium intermediate has been deeply studied. Generally, while with 3-indolymethyl acetates the nucleophilic substitutions occur exclusively at the exomethyl position, with 2-indolymethyl acetates the regiochemical outcome could be influenced by the choice of the ligand and protecting group.

Quantum-chemical calculations have been performed to provide insight into the reaction pathways confirming the key role of the palladium catalysis and highlighting the differences between the catalyzed and uncatalyzed processes.

EXPERIMENTAL SECTION

General information, experimental procedures, spectral data of starting materials, final compounds, and spectra copies of synthesized compounds are reported in the [Supporting Information](#).

General Experimental Procedure for the Reaction of *N*-Protected Indolymethyl Acetates **4 or **11** with Carbonucleophiles **5**.** In a 50 mL Carousel Tube Reactor (Radely Discovery Technology) containing a magnetic stirring bar, Pd source (0.006 mmol, 0.02 equiv) and ligand (0.012 mmol, 0.04 equiv) were dissolved in anhydrous solvent (1 mL) and stirred at room temperature for 15 min under argon. Then, *N*-protected indolymethyl acetate **4** or **11** (0.300 mmol, 1.00 equiv), carbonucleophile **5** (0.450 mmol, 1.50 equiv), and K_2CO_3 (0.450 mmol, 1.50 equiv) were added to the mixture and the reaction was stirred at 100 °C. After completion of the

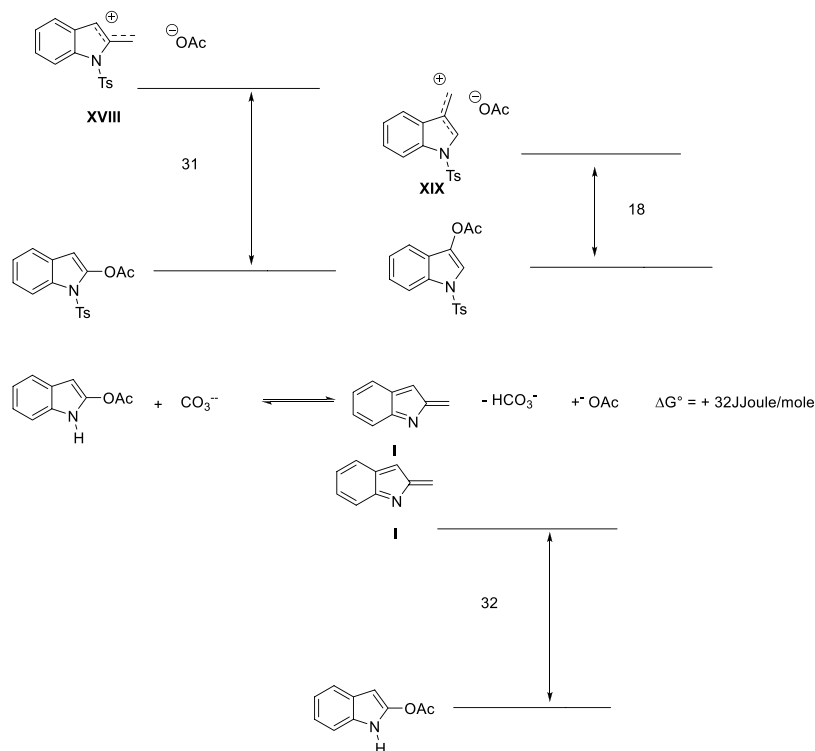


Figure 9. Standard free energy diagram (at 100 °C in DMSO) in kJ/mol.

reaction (monitored by TLC), the mixture was diluted with Et₂O and washed with a KHSO₄ solution (10% w/w) and brine (2×). The organic layer was dried over anhydrous Na₂SO₄, filtered, and concentrated under reduced pressure. The crude product was purified by flash chromatography (silica gel, *n*-hexane/AcOEt) to obtain the final products.

With *N*-protected 2-indolylmethyl acetates, depending on the nature of the carbonucleophile, the procedure is slightly modified (generation of carbanion with NaH for β -ketoesters, employment of potassium salt with β -diketones). For more details, see the [Supporting Information](#).

■ ASSOCIATED CONTENT

SI Supporting Information

The Supporting Information is available free of charge at <https://pubs.acs.org/doi/10.1021/acsomega.4c02409>.

General information, reagents and materials, typical procedures for the synthesis of starting materials and final products, characterization data, computational details, atomic coordinates, harmonic frequencies, and copies of ¹H, ¹³C, and DEPT NMR spectra ([PDF](#))

■ AUTHOR INFORMATION

Corresponding Authors

Giancarlo Fabrizi – Dipartimento di Chimica e Tecnologie del Farmaco, Sapienza, Università di Roma, 00185 Rome, Italy; Email: giancarlo.fabrizi@uniroma1.it

Antonia Iazzetti – Dipartimento di Scienze Biotecnologiche di base, Cliniche Intensivologiche e Perioperatorie, Università Cattolica del Sacro Cuore, 00168 Rome, Italy; Policlinico Universitario 'A. Gemelli' Foundation-IRCCS, Rome 00168, Italy; orcid.org/0000-0002-7792-774X; Email: antonia.iazzetti@unicatt.it

Authors

Antonio Arcadi – Dipartimento di Scienze Fisiche e Chimiche, Università degli Studi di L'Aquila, 67100 Coppito, AQ, Italy; orcid.org/0000-0001-9053-648X

Massimiliano Aschi – Dipartimento di Scienze Fisiche e Chimiche, Università degli Studi di L'Aquila, 67100 Coppito, AQ, Italy; orcid.org/0000-0003-2959-0158

Marco Chiarini – Dipartimento di Bioscienze e Tecnologie Agro-alimentari e Ambientali, Università di Teramo, 64100 Teramo, TE, Italy; orcid.org/0000-0002-2298-5467

Andrea Fochetti – Dipartimento di Chimica e Tecnologie del Farmaco, Sapienza, Università di Roma, 00185 Rome, Italy

Antonella Goggiamani – Dipartimento di Chimica e Tecnologie del Farmaco, Sapienza, Università di Roma, 00185 Rome, Italy; orcid.org/0000-0001-8339-4284

Federica Iavarone – Dipartimento di Scienze Biotecnologiche di base, Cliniche Intensivologiche e Perioperatorie, Università Cattolica del Sacro Cuore, 00168 Rome, Italy; Policlinico Universitario 'A. Gemelli' Foundation-IRCCS, Rome 00168, Italy; orcid.org/0000-0002-2074-5531

Andrea Serraiocco – Dipartimento di Chimica e Tecnologie del Farmaco, Sapienza, Università di Roma, 00185 Rome, Italy

Roberta Zoppoli – Dipartimento di Chimica e Tecnologie del Farmaco, Sapienza, Università di Roma, 00185 Rome, Italy

Complete contact information is available at: <https://pubs.acs.org/doi/10.1021/acsomega.4c02409>

Notes

The authors declare no competing financial interest.

■ ACKNOWLEDGMENTS

We gratefully acknowledge “Sapienza”, University of Rome, University of L’Aquila, the Catholic University of Sacred Heart, and PRIN project 2017 “Targeting Hedgehog pathway: virtual screening identification and sustainable synthesis of novel Smo and Gli inhibitors and their pharmacological drug delivery strategies for improved therapeutic effects in tumors” (2017SXBSX4), for financial support. M.A. would like to acknowledge prof. Nico Sanna (University of Tuscia - Viterbo - Italy) for computational facilities and for the use of the package Gaussian16.

■ REFERENCES

- (1) Kim, T.; Ha, M. W.; Kim, J. Recent Advances in Divergent Synthetic Strategies for Indole-Based Natural Product Libraries. *Molecules* **2022**, *27* (7), 2171.
- (2) Pang, Q.; Zuo, W.-F.; Zhang, Y.; Li, X.; Han, B. Recent Advances on Direct Functionalization of Indoles in Aqueous Media. *Chem. Rec.* **2023**, *23* (3), No. e202200289.
- (3) (a) Sachse, F.; Schneider, C. Brønsted Acid Catalyzed (3 + 2)-Cycloaddition of Thioketones and Indole-2-Carbinols Toward Thiazolo[3,4-a]indoles. *Adv. Synth. Catal.* **2022**, *364* (1), 77–81. (b) Zhang, Y.-C.; Jiang, F.; Shi, F. Organocatalytic Asymmetric Synthesis of Indole-Based Chiral Heterocycles: Strategies, Reactions, and Outreach. *Acc. Chem. Res.* **2020**, *53* (2), 425–446. (c) Kataja, A. O.; Masson, G. Imine and iminium precursors as versatile intermediates in enantioselective organocatalysis. *Tetrahedron* **2014**, *70* (46), 8783–8815. (d) Palmieri, A.; Petrini, M.; Shaikh, R. R. Synthesis of 3-substituted indoles via reactive alkylideneindolenine intermediates. *Organic & Biomolecular Chemistry* **2010**, *8* (6), 1259–1270. (e) Li, T.-Z.; et al. Catalytic Asymmetric (3 + 3) Cycloaddition between Different 2-Indolylmethanols. *Sci. China Chem.* **2024**, DOI: [10.1007/s11426-023-1927-3](https://doi.org/10.1007/s11426-023-1927-3). (f) Shi, Y.-C.; Yan, X.-Y.; Wu, P.; Jiang, S.; Xu, R.; Tan, W.; Shi, F. Design and Application of *m*-Hydroxybenzyl Alcohols in Regioselective (3 + 3) Cycloadditions of 2-Indolylmethanols. *Chin. J. Chem.* **2023**, *41* (1), 27–36. (g) Sheng, F.-T.; Yang, S.; Wu, S.-F.; Zhang, Y.-C.; Shi, F. Catalytic Asymmetric Synthesis of Axially Chiral 3,3'-Bisindoles by Direct Coupling of Indole Rings. *Chin. J. Chem.* **2022**, *40* (18), 2151–2160.
- (4) (a) Zhong, X.; Li, Y.; Zhang, J.; Zhang, W.-X.; Wang, S.-X.; Han, F.-S. Formal [3 + 3] cycloaddition of indol-2-yl carbinol with azadiene and the oxidative ring expansion reaction for the synthesis of indole azepinones. *Chem. Commun.* **2014**, *50* (76), 11181–11184. (b) Fu, T.-h.; Bonaparte, A.; Martin, S. F. Synthesis of β -heteroaryl propionates via trapping of carbocations with π -nucleophiles. *Tetrahedron letters* **2009**, *50* (26), 3253–3257.
- (5) (a) Patel, S. M.; P, E. P.; Bakthadoss, M.; Sharada, D. S. Photocatalytic Visible-Light-Induced Nitrogen Insertion via Dual C(sp³)–H and C(sp²)–H Bond Functionalization: Access to Privileged Imidazole-based Scaffolds. *Org. Lett.* **2021**, *23* (2), 257–261. (b) Deng, S.; Qu, C.; Jiao, Y.; Liu, W.; Shi, F. Insights into 2-Indolylmethanol-Involved Cycloadditions: Origins of Regioselectivity and Enantioselectivity. *Journal of Organic Chemistry* **2020**, *85* (18), 11641–11653. (c) Bera, K.; Schneider, C. Brønsted Acid Catalyzed [3 + 2]-Cycloaddition of Cyclic Enamides with in Situ Generated 2-Methide-2H-indoles: Enantioselective Synthesis of Indolo[1,2-*a*]-indoles. *Org. Lett.* **2016**, *18* (21), 5660–5663. (d) Bera, K.; Schneider, C. Brønsted Acid Catalyzed [3 + 2]-Cycloaddition of 2-Vinylindoles with In Situ Generated 2-Methide-2H-indoles: Highly Enantioselective Synthesis of Pyrrolo[1,2-*a*]indoles. *Chem.—Eur. J.* **2016**, *22* (21), 7074–7078. (e) Liu, C.-Y.; Han, F.-S. Organocatalytic asymmetric reaction of indol-2-yl carbinols with enamides: synthesis of chiral 2-indole-substituted 1,1-diaryllkanes. *Chem. Commun.* **2015**, *51* (59), 11844–11847. (f) Gong, Y.-X.; Wu, Q.; Zhang, H.-H.; Zhu, Q.-

- N.; Shi, F. Enantioselective construction of a 2,2'-bisindolylmethane scaffold via catalytic asymmetric reactions of 2-indolylmethanols with 3-alkylindoles. *Organic & Biomolecular Chemistry* **2015**, *13* (29), 7993–8000. (g) Qi, S.; Liu, C.-Y.; Ding, J.-Y.; Han, F.-S. Chiral phosphoramidate-catalyzed enantioselective synthesis of 2,3'-diindolylmethanes from indol-2-yl carbinols and indoles. *Chem. Commun.* **2014**, *50* (62), 8605–8608.
- (6) Arcadi, A.; Fabrizi, G.; Fochetti, A.; Ghirga, F.; Goggiamani, A.; Iazzetti, A.; Marrone, F.; Mazzocanti, G.; Serraiocco, A. Palladium-catalyzed Tsuji–Trost-type reaction of benzofuran-2-ylmethyl acetates with nucleophiles. *RSC Adv.* **2021**, *11* (2), 909–917.
- (7) Arcadi, A.; Calcaterra, A.; Chiarini, M.; Fabrizi, G.; Fochetti, A.; Goggiamani, A.; Iazzetti, A.; Marrone, F.; Marsicano, V.; Serraiocco, A. Synthesis of Indole/Benzofuran-Containing Diarylmethanes through Palladium-Catalyzed Reaction of Indolylmethyl or Benzofuranylmethyl Acetates with Boronic Acids. *Synthesis* **2022**, *54* (03), 741–753.
- (8) Arcadi, A.; Berden, G.; Ciogli, A.; Corinti, D.; Crestoni, M. E.; De Angelis, M.; Fabrizi, G.; Goggiamani, A.; Iazzetti, A.; Marrone, F.; Marsicano, V.; Oomens, J.; Serraiocco, A. Reactivity of Indolylmethylacetates with N, O, and S Soft Nucleophiles: Evidence of 2-Alkylideneindolenines and 3-Alkylideneindoleninium Generation by ESI-MS and IRMPD Spectroscopy. *Eur. J. Org. Chem.* **2022**, *2022* (43), e202201166.
- (9) Goggiamani, A.; Arcadi, A.; Ciogli, A.; De Angelis, M.; Dessalvi, S.; Fabrizi, G.; Iavarone, F.; Iazzetti, A.; Sferrazza, A.; Zoppoli, R. Synthesis of 3-substituted 2,3-dihydropyrazino[1,2-a]indol-4(1H)-ones by sequential reactions of 2-indolylmethyl acetates with α -amino acids. *RSC Adv.* **2023**, *13* (15), 10090–10096.
- (10) Iazzetti, A.; Arcadi, A.; Dessalvi, S.; Fabrizi, G.; Goggiamani, A.; Marrone, F.; Serraiocco, A.; Sferrazza, A.; Ullah, K. Synthesis of Polysubstituted 1,2-Dihydro-3H-pyrrolo[1,2-a]indol-3-ones through Domino Palladium-Catalyzed Reactions of Indol-2-ylmethyl Acetates with 1,3-Dicarbonyl Derivatives. *Catalyst* **2022**, *12* (12), 1516.
- (11) (a) Primault, G.; Legros, J.-Y.; Fiaud, J.-C. Palladium-catalyzed benzylic-like nucleophilic substitution of benzofuran-, benzothiophene- and indole-based substrates by dimethyl malonate anion. *J. Organomet. Chem.* **2003**, *687* (2), 353–364. (b) Yang, L.; Chen, X.; Ni, K.; Li, Y.; Wu, J.; Chen, W.; Ji, Y.; Feng, L.; Li, F.; Chen, D. Proton-exchanged montmorillonite-mediated reactions of hetero-benzyl acetates: Application to the synthesis of Zafirlukast. *Tetrahedron letters* **2020**, *61* (29), 152123.
- (12) Kamer, P. C. J.; van Leeuwen, P. W. N. M.; Reek, J. N. H. Wide Bite Angle Diphosphines: Xantphos Ligands in Transition Metal Complexes and Catalysis. *Acc. Chem. Res.* **2001**, *34* (11), 895–904.
- (13) Yang, D.; Zhou, Y.; Xue, N.; Qu, J. Synthesis of Trifluoromethyl Ketones via Tandem Claisen Condensation and Retro-Claisen C–C Bond-Cleavage Reaction. *Journal of Organic Chemistry* **2013**, *78* (8), 4171–4176.
- (14) Arcadi, A.; Calcaterra, A.; Fabrizi, G.; Fochetti, A.; Goggiamani, A.; Iazzetti, A.; Marrone, F.; Mazzocanti, G.; Serraiocco, A. One-pot synthesis of dihydroquinolones by sequential reactions of *o*-amino-benzyl alcohol derivatives with Meldrum's acids. *Organic & Biomolecular Chemistry* **2022**, *20* (15), 3160–3173.
- (15) Duchemin, N.; Cattoen, M.; Gayraud, O.; Anselmi, S.; Siddiq, B.; Buccafusca, R.; Daumas, M.; Ferey, V.; Smietana, M.; Arseniyadis, S. Direct Access to Highly Enantioenriched α -Branched Acrylonitriles through a One-Pot Sequential Asymmetric Michael Addition/Retro-Dieckmann/Retro-Michael Fragmentation Cascade. *Org. Lett.* **2020**, *22* (15), 5995–6000.
- (16) Chai, J. D.; Head-Gordon, M. Systematic optimization of long-range corrected hybrid density functionals. *J. Chem. Phys.* **2008**, *128* (8), 084106.
- (17) Hay, P. J.; Wadt, W. R. Ab initio effective core potentials for molecular calculations. Potentials for K to Au including the outermost core orbitals. *J. Chem. Phys.* **1985**, *82* (1), 299–310.
- (18) Tomasi, J.; Mennucci, B.; Cammi, R. Quantum Mechanical Continuum Solvation Models. *Chem. Rev.* **2005**, *105* (8), 2999–3094.
- (19) Frisch, M. J.; Trucks, G. W.; Schlegel, H. B.; Scuseria, G. E.; Robb, M. A.; Cheeseman, J. R.; Scalmani, G.; Barone, V.; Petersson, G. A.; Nakatsuji, H.; Li, X.; Caricato, M.; Marenich, A.; Bloino, J.; Janesko, B. G.; Gomperts, R.; Mennucci, B.; Hratchian, H. P.; Ortiz, J. V.; Izmaylov, A. F.; Sonnenberg, J. L.; Williams-Young, D.; Ding, F.; Lipparini, F.; Egidi, F.; Goings, J.; Peng, B.; Petrone, A.; Henderson, T.; Ranasinghe, D.; Zakrzewski, V. G.; Gao, J.; Rega, N.; Zheng, G.; Liang, W.; Hada, M.; Ehara, M.; Toyota, K.; Fukuda, R.; Hasegawa, J.; Ishida, M.; Nakajima, T.; Honda, Y.; Kitao, O.; Nakai, H.; Vreven, T.; Throssell, K.; Montgomery, J. A., Jr.; Peralta, J. E.; Ogliaro, F.; Bearpark, M.; Heyd, J. J.; Brothers, E.; Kudin, K. N.; Staroverov, V. N.; Keith, T.; Kobayashi, R.; Normand, J.; Raghavachari, K.; Rendell, A.; Burant, J. C.; Iyengar, S. S.; Tomasi, J.; Cossi, M.; Millam, J. M.; Klene, M.; Adamo, C.; Cammi, R.; Ochterski, J. W.; Martin, R. L.; Morokuma, K.; Farkas, O.; Foresman, J. B.; Fox, D. J. *Gaussian 09*, Revision A.02; Gaussian, Inc.: Wallingford, CT, 2016.